Journal of Hazardous Materials 215–216 (2012) 272–279

Contents lists available at SciVerse ScienceDirect

Journal of Hazardous Materials

journal homepage: www.elsevier.com/locate/jhazmat

Fabrication of novel magnetic chitosan grafted with graphene oxide to enhance adsorption properties for methyl blue

Lulu Fan, Chuannan Luo*, Xiangjun Li, Fuguang Lu, Huamin Qiu, Min Sun

Key Laboratory of Chemical Sensing & Analysis in Universities of Shandong (University of Jinan), School of Chemistry and Chemical Engineering, University of Jinan, Jinan 250022, China

ARTICLE INFO

Article history:
Received 24 November 2011
Received in revised form 7 February 2012
Accepted 25 February 2012
Available online 3 March 2012

Keywords:
Magnetic chitosan
Graphene oxide
Methyl blue
Adsorption
Langmuir

ABSTRACT

A novel magnetic composite bioadsorbent composed of magnetic chitosan and graphene oxide (MCGO) was prepared as the magnetic adsorbent. The morphology, chemical structure and magnetic property of the MCGO were characterized by Fourier transform infrared spectrometer (FT-IR), X-ray diffraction (XRD) and Scanning electronic microscope (SEM), respectively. Adsorption of methyl blue (MB) onto MCGO was investigated with respect to pH, adsorption time, initial MB concentration and temperature. Kinetics data and adsorption isotherm, obtained at the optimum pH 5.3, were better fitted by pseudo-second-order kinetic model and by Langmuir isotherm, respectively. The values of activation parameters such as free energy (ΔG, $-0.74 \sim -1.46$ kJ mol^{-1}), enthalpy (ΔH, -10.28 kJ mol^{-1}) and entropy (ΔS, -36.35 J mol^{-1} K^{-1}) were determined, respectively, indicating that the adsorption was spontaneous, favorable and exothermic process in nature. Moreover, the MCGO was stable and easily recovered, the adsorption capacity was about 90% of the initial saturation adsorption capacity after being used four times.

© 2012 Elsevier B.V. All rights reserved.

1. Introduction

Dyes are important chemicals widely used in pharmaceuticals, rubbers, pesticides, varnishes and dyestuffs and so on. Dyeing effluent has a serious environmental impact because disposal of this effluent into the receiving water body causes damage to aquatic biota and humans by mutagenic and carcinogenic effects. Thus, the removal of dyes from waste water is important for risk assessment. Now, various removal methods have been obtained such as sorption [1–3], chemical coagulation [4], liquid membrane separation [5], electrolysis [6], biological treatments [7], oxidation [8] and some other processes [9].

However, these processes vary in their effectiveness, cost and environmental impact [10]. Adsorption is a more competitive treatment process for dye removal because of its simplicity, high efficiency, and wide-ranging availability [11,12]. Hence, there is a need to search for adsorbents that are more effective, since the water treatment industry requires ecofriendly, highly effective and low cost adsorbents that are available in tonnage quantities.

Natural biomasses as adsorbents are drawing more and more attentions due to their biodegradability, biocompatibility and renewability [13,14]. Chitosan exhibits a high adsorption capacity toward many classes of dyes especially anionic dyes because of its high amino and hydroxyl functional group content [15]. Due to its accessibility, high effectivity and no harmful by-product, it is often chosen as an bioadsorbent for the removal or the recovery of hazardous dyes, proteins, heavy metals and so on [16–19]. However, there are some disadvantages of powdery chitosan baffling its practical applications, such as chitosan dissolves below pH 5.5 and it is difficult to be separated and recovered except by high speed centrifugation and filter [20]. Thus, it is significant to explore novel environment friendly chitosan-based bioadsorbents, which possess higher adsorption capacity and excellent separation property.

Magnetic fluids have the capability to treat large amounts of wastewater within a short time and can be conveniently separated from wastewater; at the same time, they could be tailored by using functionalized polymers, novel molecules, or inorganic materials to impart surface reactivity. Coating chitosan with magnetic fluids is a new method to expand function of the chitosan, and the method has been reported that it can improve the surface area for adsorption and reduce the required dosage for the adsorption of dyes [14]. The preparation of magnetic chitosan is schematically illustrated in Scheme 1A.

Graphene, a fascinating two dimensional carbon-based material possessing atomic thickness, has attracted considerable attention world over, since the report of Novoselov et al. [21]. This excitement is greatly attributed to its excellent mechanical and physicochemical properties [22]. Recent researches have indicated that GO proved to be a promising material to adsorb dyes and support

* Corresponding author. Fax: +86 531897360651.
E-mail addresses: fanlu1949@126.com (L. Fan), chm_luocn@ujn.edu.cn (C. Luo).

0304-3894/$ – see front matter © 2012 Elsevier B.V. All rights reserved.
doi:10.1016/j.jhazmat.2012.02.068

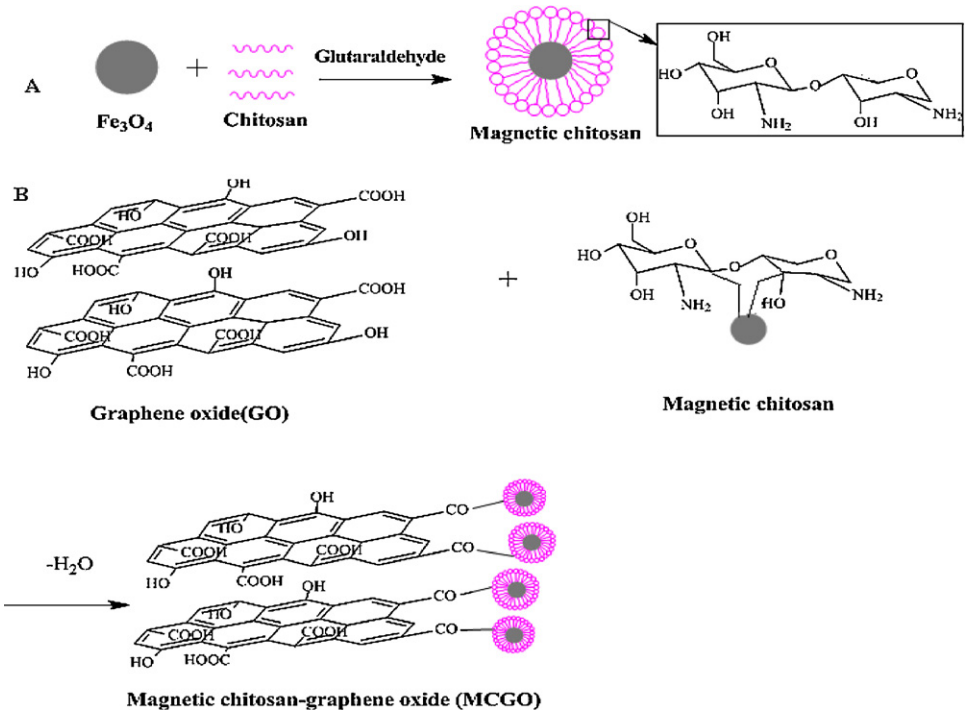

Scheme 1. Schematic depiction of the formation of magnetic chitosan (A) and MCGO (B).

for catalyst due to their extraordinary mechanical strength and relatively large specific area [9,23]. Based on favorable adsorption properties of chitosan and inherent properties of GO some researchers have explored the possibility of chitosan-GO composite as bioadsorbents[24]. Where the carboxyl group of GO chemically reacts with the amine group of chitosan (CS) with consequent formation of chemical bond between GO and biopolymer (chitosan).

However, magnetic chitosan strengthened by graphene oxide has not been synthesized and applied in removing MB from aqueous solution. The preparation of MCGO is schematically illustrated in Scheme 1B.

In this work, the aim was to explore and prepare MCGO composite bioadsorbent with higher adsorption capacity and excellent separation properties. Methyl blue (MB) with large and complicated structures was selected as model pollutant to evaluated the adsorption characteristics of MCGO under laboratory conditions. This information will be useful for further research and practical applications of the novel bioadsorbent in dyeing wastewater treatment. The application of MCGO for removal of MB with the help of an external magnetic field is shown in Scheme 2.

2. Materials and methods

2.1. Materials

Chitosan with 80 mesh, 96% degree of deacetylation and average-molecular weight of 6.36×10^5 was purchased from Qingdao Baicheng Biochemical Corp. (China). $FeCl_2{\cdot}4H_2O$ and $FeCl_3{\cdot}6H_2O$ were purchased from Damao Chemical Agent Company (Tijin, China). The reagents 1-ethyl-3-(3-dimethylaminoprophy) carbondiimide hydrochloride (EDC), N-hydroxyl succinimide (NHS), sodium hydroxide, glutaradehyde and acetic acid were Aldrich products. All other reagents used in this study were analytical grade, and distilled or double distilled water was used in the preparation of all solutions.

2.2. Preparation of magnetic chitosan

0.6268 g of $FeCl_2{\cdot}4H_2O$, 1.7312 g of $FeCl_3{\cdot}6H_2O$ and 25 mL of double distilled water were dropwise to ammonia solution, which was purged with nitrogen and stirred in a water bath at 90 °C for 3 h. Magnetic particles used in the chitosan coating were obtained by magnetic separation.

0.3 g chitosan was dissolved in 30 mL 3% of acetic solution to give a final concentration of 1.5% (w/v). 0.1 g magnetic particles were added in the chitosan solution in a four-neck rounded bottom flask. 2.0 mL of pure glutaraldehyde was added into reaction flask to mix with the solution and was stirred at 60 °C for 2 h. The precipitate was washed with petroleum ether, ethanol and distilled water in turn until pH was about 7. Then, the precipitate was dried in a vacuum oven at 50 °C. The obtained product was magnetic chitosan.

2.3. Synthesis of graphene oxide(GO)

Graphene oxide (GO) was prepared from purified natural graphite by the modified Hummers method [25]. Briefly, natural graphite and potassium permanganate were stirred with the mixed acid (H_2SO_4:HNO_3 = 9:1) for 12 h at 60 °C. Then, hydrogen peroxide was added in the mixed liquor and stirred for 1 h resulting in bright yellow colored end product [23]. This material was washed with 2 M HCl till bisulfate ions were removed and then with copious amount of water till the solution became neutral. Subsequently, the GO was gotten by centrifuging, and was dried in vacuum desiccator.

2.4. Preparation of MCGO

A GO dispersion was prepared by sonicating GO for 3 h in ultrapure water. A solution of 0.05 M EDC and 0.05 M NHS was added to the GO dispersion with continuous stirring for 2 h in order to activate the carboxyl groups of GO [26]. The pH of the resulting solution was maintained at 7.0 using dilute sodium hydroxide. 0.1 g of magnetic chitosan and the activated GO solution were added in a flask and dispersed in distilled water by ultrasonic dispersion

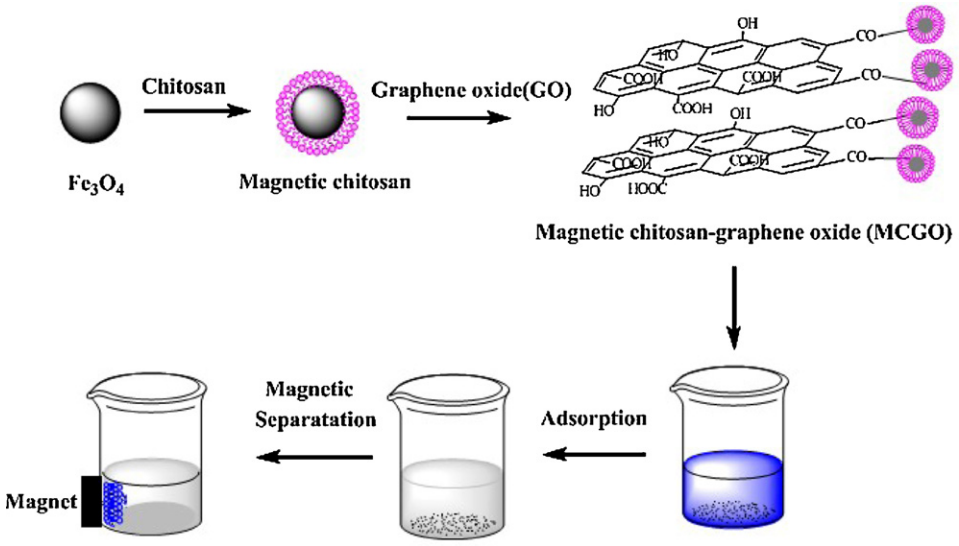

Scheme 2. Synthesis of MCGO and their application for removal of MB with the help of an external magnetic field.

for 10 min. After ultrasonic dispersion, the mixed solutions were stirred at 60 °C for 2 h. The precipitate was washed with 2% (w/v) NaOH and distilled water in turn until pH was about 7. Then, the obtained product was collected by the aid of an adscititious magnet and dried in a vacuum oven at 50 °C. The obtained product was MCGO.

2.5. Adsorption experiments

Batch adsorption experiments were carried out by using the MCGO as the adsorbent. All batch adsorption experiments were performed on a SHA-C shaker (Changzhou, China) with a shaker speed of 150 rpm until the system reached equilibrium. Typically, a 25 mL solution of known MB concentration and 0.015 g of MCGO were added into 100 mL glass flasks and then shook under 30 ± 0.2 °C. At the completion of preset time intervals, the dispersion was drawn and separated immediately by the aid of a magnet to collect the bioadsorbent. Residual MB concentration in supernatant was measured using a spectrophotometer (722-type, Shanghai Analytical Instruments General Factory, China). The absorbance is $\max_{MB}$ = 610 nm. The adsorption amount and adsorption rate are calculated based on the difference in the MB concentration in the aqueous solution before and after adsorption, according to the following equation:

$$Q = \frac{(C_0 - C_e)V}{W}, \quad E = \frac{(C_0 - C_e)}{C_0} \times 100\%$$

where C_0 and C_e are the initial and equilibrium concentrations of MB in milligrams per liter, respectively, V is the volume of MB solution, in liters, and W is the weight of the MCGO used, in grams.

2.6. Characterization of the samples

Microscopic observation of samples was carried out by using a scanning electron microscope (S-2500, Japan Hitachi). FT-IR spectra of samples were recorded with KBr pellet in the range of 4000–400 cm^{-1} on FTIR spectra were measured on a Nicolet, Magna 550 spectrometer. Wide angle X-ray diffraction (WAXRD) patterns were recorded by a D8 ADVANCE X-ray diffraction spectrometer (Bruker, German) with a Cu Kα target at a scan rate of 0.02° $2\theta\,s^{-1}$ from 10° to 80°. The Brunauer–Emmett–Teller (BET) surface area and the pore size distribution of the composite were measured using N_2 adsorption and desorption (QUADRASORBSI, Quantachrome, USA) at 77 K over a relative pressure ranging from 0.0955 to 0.993. DSC and TGA of samples were performed with Setaram Setsys 16 TG/DTA/DSC thermal analyzer (France) under a dynamic N_2 atmosphere from 25 °C to 800 °C with heating rate of 2 °C min^{-1}.

2.7. Replication of batch experiment

Each batch adsorption experiment above was conducted in triplicates to obtain reproductive results with error <5%. In the case of deviation larger than 5%, more tests were carried out. The experimental data could be reproduced with an accuracy greater than 95%. All the data of batch adsorption experiments listed in Section 3 are the average values of three tests.

3. Results and discussion

3.1. Characterization of MCGO

The FTIR pattern of GO, which is shown in Fig. 1A, reveals the presence of the oxygen-containing functional groups. The peaks at 1071, 1380, 1630 correspond to C—O—C stretching vibrations, C—OH stretching, C—C stretching mode of the sp2 carbon skeletal network, respectively, while peaks located at 1730, and 3440 cm^{-1} correspond to C—O stretching vibrations of the —COOH groups, and O—H stretching vibration, respectively[26]. As shown in Fig. 1B, there are two characteristic absorbance bands centered at 1636 and 1597 cm^{-1}, which correspond to the C—O stretching vibration of —NHCO— (amide I) and the N—H bending of $-NH_2$, respectively [27]. However, in the case of GO grafted derivatives, it can be distinctly observed that the $-NH_2$ absorbance band has shifted to a lower value and the intensity of acetylated amino group NHCO— (amide I) has increased, which proves that $-NH_2$ groups on the CS chains have been reacted with the —COOH groups of GO and therefore have been converted to —NHCO— graft points. In addition, 580 cm^{-1} is the characteristic peak of Fe_3O_4. These indicated that GO was successfully grafted on magnetic chitosan.

XRD patterns of pure Fe_3O_4, magnetic chitosan and MCGO are shown in Fig. 2, indicating the existence of iron oxide particles (Fe_3O_4), which has magnetic properties and can be used for the magnetic separation. The XRD analysis results of pure Fe_3O_4 magnetic chitosan and MCGO were mostly coincident. Six characteristic peaks for Fe_3O_4 (2θ = 30.1, 35.5, 43.3, 53.4, 57.2 and 62.5), marked

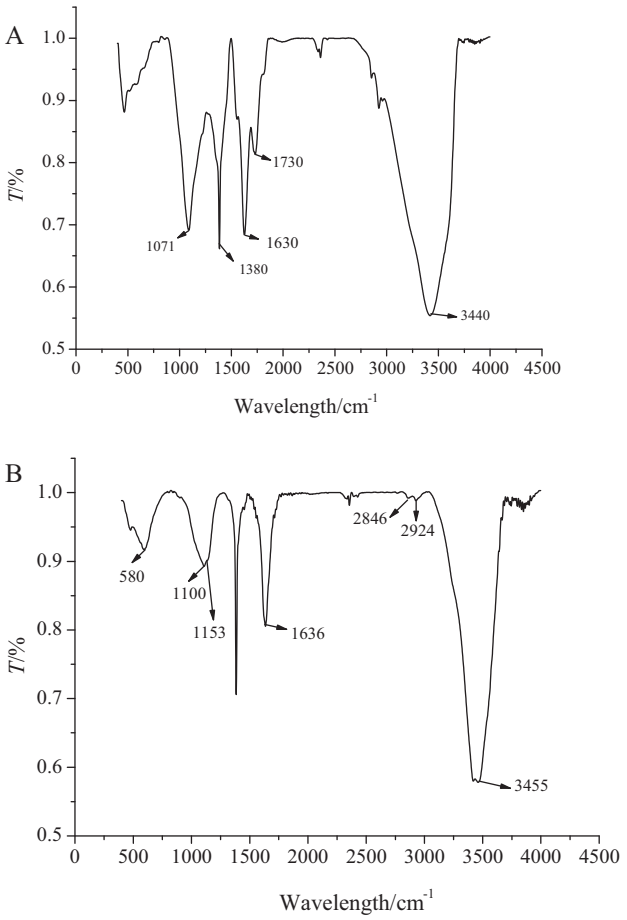

Fig. 1. IR spectra of GO (A) and MCGO (B).

by their indices ((2 2 0), (3 1 1), (4 0 0), (4 2 2), (5 1 1), and (4 4 0)), were observed in samples.

Fig. 3A shows the typical SEM images of GO obtained by a modified Hummers method. The GO presents the sheet-like structure with the large thickness, smooth surface, and wrinkled edge. After the combination with magnetic chitosan to form the MCGO composite (Fig. 3B), the MCGO had a much rougher surface, revealing that many small magnetic chitosan had been assembled on the surface of GO layers with a high density.

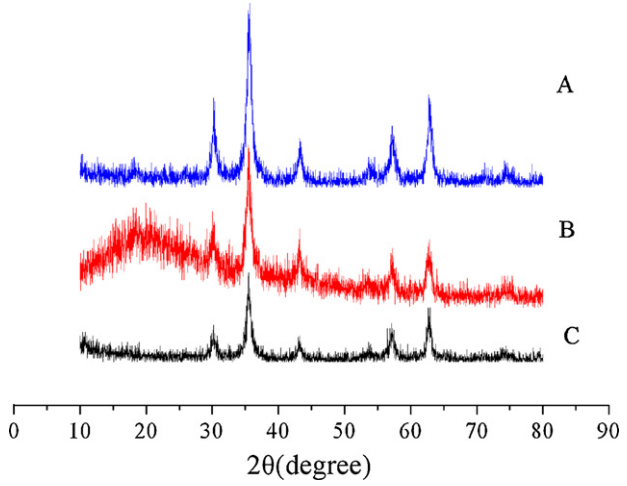

Fig. 2. XRD pattern of pure Fe_3O_4 (A), magnetic chitosan (B) and MCGO (C).

The BET surface area and pore volume estimated from Barret–Joyner–Halenda (BJH) analysis of the isotherms were determined to be 392.5 m^2/g and 0.3852 cm^3/g, respectively. Also, the average of the pore size distribution is 2.587 nm. The value of the pore diameter indicates that MCGO is a mesoporous material. The average particle size was 200 nm. In addition, from 25 °C to 158 °C, there was a weight loss of about 13.24% corresponding to water loss in biomaterials and an extremum of endothermic peak in DSC curve appeared at 80 °C.

3.2. Effect of pH value on adsorption

The pH of aqueous solution was an important parameter that determined the adsorption capacity onto MCGO. The experiments were carried out in pH range 0.5–7.6 and the results are illustrated in Fig. 4. The dye uptake was increased as pH increased from 0.5 to 4.5. Above pH 6.5, the MCGO displayed a sharp decrease in the uptake value as pH increased. Therefore, the optimum pH range for MB adsorption onto MCGO bioadsorbents was 4.5–6.5.

The mechanisms of the adsorption process of MB on the MCGO were due to be the ionic interactions of the colored dye with the amino groups of the MCGO. In aqueous solution, the MB was first dissolved and the sulfonate groups of MB (D-SO_3Na) dissociate and were converted to anionic dye ions.

$$\text{D-SO}_3\text{Na} \leftrightarrow \text{D-SO}_3^- + \text{N}_a^+$$

The amino groups of MCGO were protonated under acidic conditions according to the following reaction:

$$\text{R-NH}_2 + \text{H}^+ \leftrightarrow \text{R-NH}_3^+$$

In addition, under acidic conditions (pH < 4.5), the sulfonate groups (D-SO_3^-) combined with H^+, which decreased the adsorption capacity of MB, according to the following reaction:

$$\text{D-SO}_3^- + \text{H}^+ \leftrightarrow \text{D-SO}_3\text{H}$$

As a result, the sorption processed proceeds through electrostatic interaction between the two counterions (R-NH_3^+ and D-SO_3^-) [29]:

$$\text{R-NH}_3^+ + \text{D-SO}_3^- \leftrightarrow \text{R-NH}_3^+ \cdots \text{SO}_3\text{-D}$$

In addition, at pH above 6.5, the number of protonated $-NH_2$ groups were decrease and excessive hydroxyl ions of MCGO might compete with the dye anions and hence obvious reductions in dye uptake were observed.

3.3. Adsorption kinetics

Adsorption is a physicochemical process that involves mass transfer of a solute from liquid phase to the adsorbent's surface [20]. Kinetic study provided important information about the mechanism of MB adsorption onto MCGO, which was necessary to depict the adsorption rate of adsorbent and control the residual time of the whole adsorption process. The adsorption kinetics of MB onto MCGO was investigated with the help of two kinetic models, namely the Lagergren pseudo-first-order and pseudo-second-order model. The Lagergren rate equation is one of the most widely used adsorption rate equations for the adsorption of solute from a liquid solution. The pseudo-first-order kinetic model is expressed by the following equation:

$$\ln(Q_e - Q_t) = \ln Q_e - K_1 t$$

where Q_e and Q_t are the amount adsorbed in mg g^{-1} at equilibrium, time 't' in min, and K_1 is the rate constant of adsorption (min^{-1}). The values of experimental Q_e do not agree with the calculated ones, obtained from the linear plots (Fig. 5A), and the values of correlation

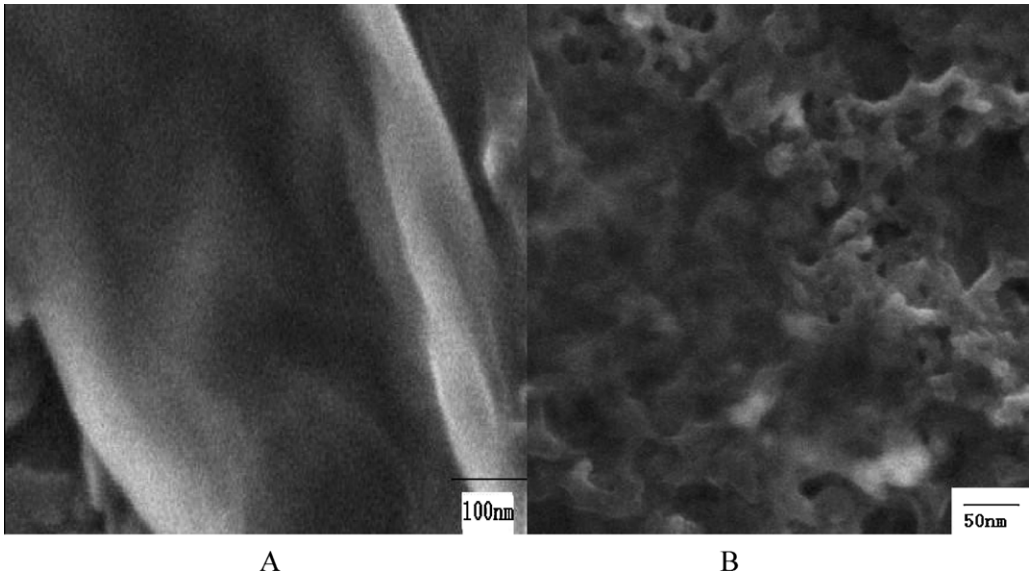

Fig. 3. SEM images of GO (A) and MCGO (B).

Table 1
Adsorption kinetic parameters of MB onto MCGO.

Initial conc. C_0 (mg L^{-1})	Pseudo-first-order		R^2	Pseudo-second-order			R^2
	K_1 (min^{-1})	$Q_{e,cal}$ (mg g^{-1})		$Q_{e,cal}$ (mg g^{-1})	K_2, g/(mg. Min)	$Q_{e,exp}$ (mg g^{-1})	
60	0.001	7.09	0.72	9.89	0.096	11.02	0.991
200	0.0032	3.63	0.61	79.94	0.012	81.56	0.993

coefficient (R^2) are relatively low for most of the adsorption data (Table 1). This shows that the adsorption process may not be the correct fit to the first-order rate equation. Another kinetic model is pseudo-second-order model, which is expressed by:

$$\frac{t}{Q_t} = \frac{1}{K_2 Q_e^2} + \frac{t}{Q_e}$$

where K_2 is the rate constant for the pseudo-second-order adsorption process. The linear plots of t/Q_t versus t show good agreement between experimental and calculated Q_e values at different initial concentrations (Fig. 5B). The correlation coefficient (R^2) (Table 1) for the pseudo-second-order adsorption model has high value (>99%) for adsorbent. These facts suggest that the pseudo-second-order adsorption mechanism is predominant.

Intraparticle diffusion model is described using the equation [23]:

$$Q_t = K_p t^{0.5} + C$$

where K_p is intraparticle diffusion constant (mg g^{-1} min$^{-0.5}$). This can be obtained from plot of Q_t versus $t^{0.5}$. The intercept that gives constant 'C' indicates whether controlling step is intraparticle diffusion or not. If $C \neq 0$, the adsorption mechanism is quite complex. If $C = 0$, adsorption kinetics is only controlled by intraparticle diffusion. In the studies, C is always a non-zero value revealing that the adsorption process is not controlled only by intraparticle diffusion but involves complex mechanism pathway, including the mainly chemisorption process of chitosan and mainly physisorption process of GO.

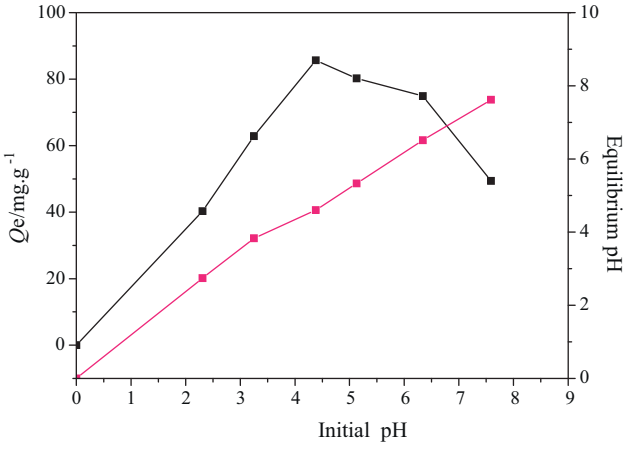

Fig. 4. Effect of pH on the adsorption capacity (initial concentration, 200 mg L^{-1}; temperature, 303 K; contact time, 60 min). Black points: Q_e versus initial pH values; red points: equilibrium pH values versus initial pH values.

3.4. Evaluation of adsorption isotherm models

The adsorption isotherm Langmuir has been used to fit the experimental adsorption data for MB on MCGO. The Langmuir adsorption isotherm is based on the assumption that adsorption takes place on homogeneous surface. The equation can be expressed as:

$$\frac{C_e}{Q_e} = \frac{1}{K_L Q_0} + \frac{C_e}{Q_0}$$

where C_e is the equilibrium concentration of MB in solution (mg L^{-1}), Q_e is the adsorbed value of MB at equilibrium concentration (mg g^{-1}), Q_0 the maximum adsorption capacity (mg g^{-1}), and K_L is the Langmuir binding constant, which is related to the energy of adsorption. Plotting C_e/Q_e against C_e gives a straight line with slope and intercept equal to $1/Q_0$ and $1/(K_L Q_0)$, respectively. It is described in Fig. 6.

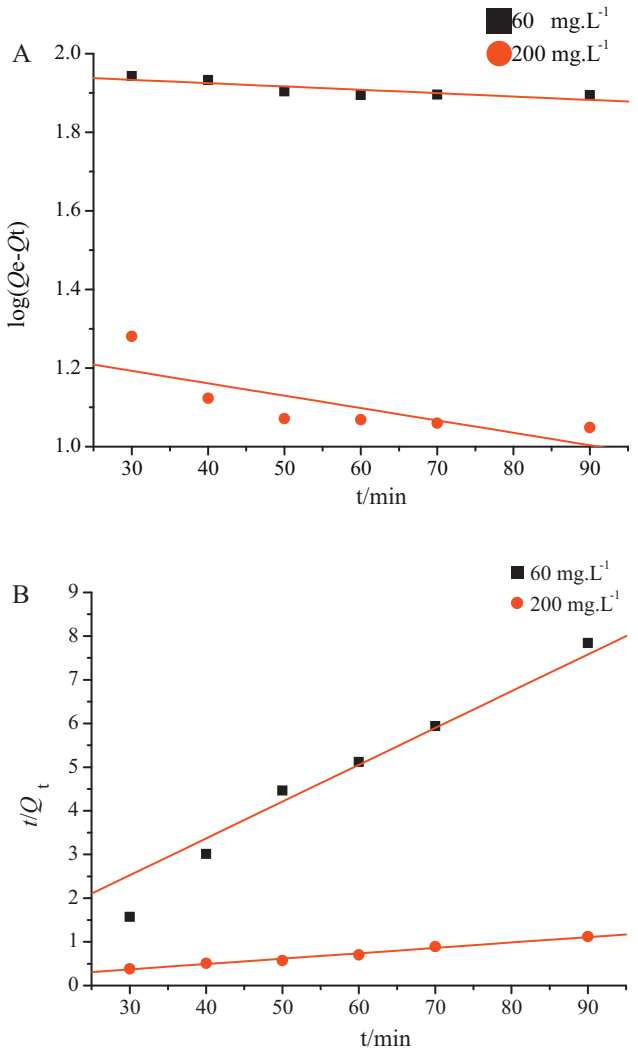

Fig. 5. Pseudo-first-order kinetic plots for the adsorption of MB (A), and pseudo-second-order kinetics for adsorption of MB (B) (pH 5.3, temperature: 303 K).

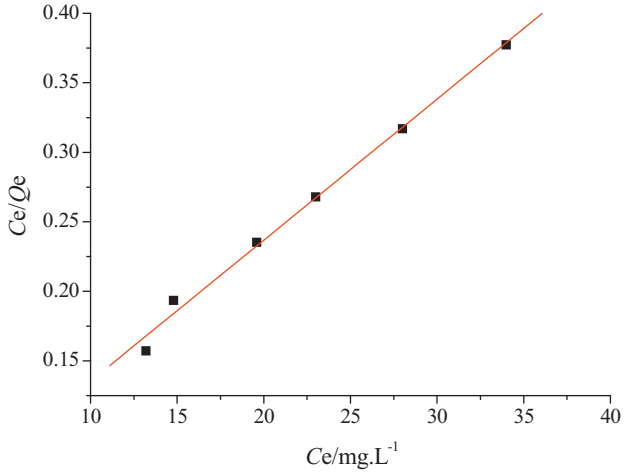

Fig. 6. The linear dependence of C_e/Q_e on C_e (pH, 5.3; temperature, 303 K; contact time, 60 min).

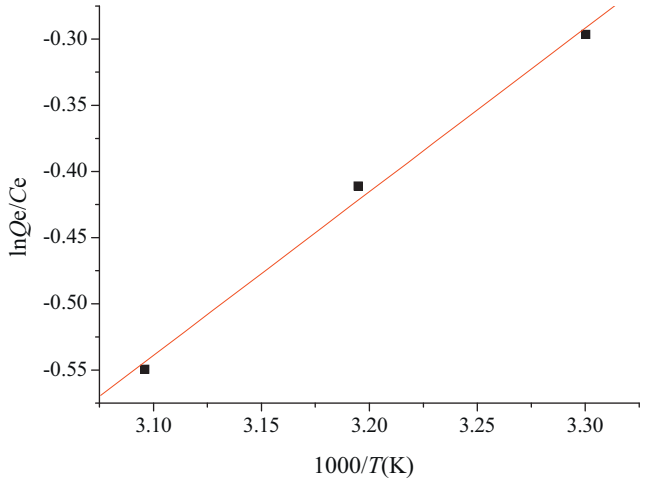

Fig. 7. Van't Hoff plots for the adsorption of MB onto MCGO.

By calculating, the results are as follows:

$$\frac{C_e}{Q_e} = 0.01015C_e + 0.03389\ (R^2 = 0.9962),\ Q_0 = 98.52\ \text{mg g}^{-1},\ K_L = 0.3\ \text{L mg}^{-1}$$

The values of Q_0 obtained from Langmuir curves are mainly consistent with that experimentally obtained (95.31 mg g^{-1}), indicating that the adsorption process is mainly monolayer. This suggests that the surfaces of MCGO behave homogeneous though three different functional groups (carboxyl, hydroxyl, and epoxy functional groups) are present [23]. The chelation adsorption mechanism for MB may give controlled monolayer adsorption.

Furthermore, the essential characteristics of the Langmuir isotherm can be described by a separation factor, which is defined by the following equation:

$$R_L = \frac{1}{1 + K_L C_e}$$

The value of R_L indicates the shape of the Langmuir isotherm and the nature of the adsorption process. It is considered to be a favorable process when the value is within the range 0–1. In the study, the value of R_L calculated for the initial concentrations of MB was 0.016. Since the result is within the range of 0–1, the adsorption of MB onto adsorbent appears to be a favorable process. In addition, the low R_L values (<0.1) implied that the interaction of MB with MCGO might be relatively strong.

3.5. Effect of temperature on adsorption

To determine the effect of temperature on MB adsorption, adsorption experiments were also conducted at 303, 313 and 323 K. The observed decrease in both values of $1/T$ and $\ln(Q_e/C_e)$ with elevated temperature indicates the exothermic nature of the adsorption process. The values of $\ln(Q_e/C_e)$ at different temperatures were treated according to Van't Hoff equation:

$$\ln\left(\frac{Q_e}{C_e}\right) = \frac{-\Delta H}{RT} + \frac{\Delta S}{R},$$

R is the universal gas constant (8.314 J/mol K) and T is the absolute temperature (in Kelvin). Plotting $\ln(Q_e/C_e)$ against $1/T$ gives a straight line with slope and intercept equal to $-\Delta H/R$ and $\Delta S/R$, respectively. It is described in Fig. 7.

The negative value of ΔH (Table 2) shows exothermic nature of adsorption process. The adsorption was favored at lower

Table 2
Thermodynamic parameters at different temperatures.

T/K	ΔG (kJ mol^{-1})	ΔH (kJ mol^{-1})	ΔS (J mol K^{-1})
303	−0.735	−10.28	−36.35
313	−1.098		
323	−1.462		

Table 3
Maximum adsorption capacities for the adsorption of MB onto various adsorbents.

Adsorbent	Adsorption capacity (mg g^{-1})	Reference
Natural chitosan membranes	46.23	This work
Magnetic chitosan	60.4	This work
GO	43.5	This work
MCGO	95.16	This work
Activated charcoal	25.25	[30]
Graphene	50	[9]

temperature and MB molecules were orderly adsorbed on the surface of MCGO. Gibbs free energy of adsorption (ΔG) was calculated from the following relation:

$$\Delta G = \Delta H - T\Delta S$$

The negative value of ΔG (Table 2) indicates that the adsorption reaction was spontaneous at 303, 313 and 323 K.

3.6. Effect of recycling adsorbents on MB adsorption

Desorption studies were performed to elucidate the mechanism of adsorption and reuse the adsorbents. Such adsorbent has higher adsorption capability as well as better desorption property which will reduce the overall cost for the adsorbent.

To evaluate the possibility of regeneration and reusability of MCGO as an adsorbent, the desorption experiments were performed. Desorption of MB from MCGO was demonstrated using three different eluents, namely 0.5 mol/L HCl, 0.5 mol/L NaOH, and H_2O. It is found that the desorption percentages of HCl, NaOH and H_2O were 5.1, 95.01 and 1.4%, respectively. The 0.5 mol/L NaOH was the optimum eluent.

The effect of five consecutive adsorption–desorption cycles was studied, and the results are shown in Fig. 8. It is shown in Fig. 8 that the adsorption capacity of MB on the adsorbents decreased slowly with increasing cycle number. The percentage adsorption remained steady at about 90% in the first four cycles, and then the adsorption capacity of MB decreased. At the five regeneration cycle, the adsorption remained at 75%. These results show that the adsorbents can be recycled for MB adsorption with 0.5 mol/L NaOH, and the adsorbents can be reused. This could be ascribed to the fact that, in the basic solution, the positively charged amino groups were deprotonated and the electrostatic interaction between MCGO and dye molecules became much weaker.

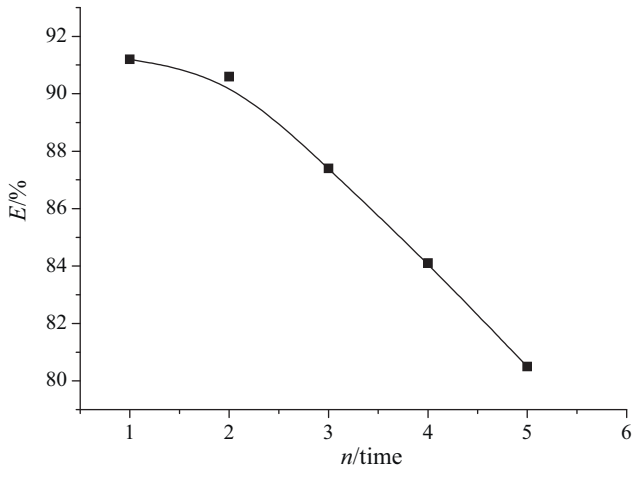

Fig. 8. Effect of recycling adsorbents on MB adsorption (pH, 5.3; initial concentration, 200 mg L^{-1}; temperature, 303 K; contact time, 60 min).

4. Conclusions

In summary, MCGO composite was prepared and characterized. The MCGO acted as a good adsorbent to adsorb MB from aqueous solutions. MCGO had higher adsorption capacity (Table 3) for MB due to the introduction of GO compared with the magnetic chitosan (Table 3). The adsorption of MB on MCGO was strongly dependent on pH and ionic strength, indicating an ion exchange mechanism. The adsorption followed pseudo-second-order kinetics, and the equilibrium data were well fitted with the Langmuir isotherms. The negative ΔG indicated that the adsorption was a spontaneous process. Thus, the novel MCGO has a great potential to be used as environmentally friendly and economical bioadsorbent for the removal of dyes from aqueous solution due to the efficient and fast adsorption process, as well as simple and convenient magnetic separation.

Acknowledgment

This work was supported by the Shandong Provincial Natural Science Foundation (Y2008B53).

References

[1] E.I. Unuabonah, K.O. Adebowale, F.A. Dawodu, Equilibrium, kinetic and sorber design studies on the adsorption of aniline blue dye by sodium tetraborate-modified kaolinite clay adsorbent, J. Hazard. Mater. 157 (2008) 397–409.
[2] J.Y. Chen, W. Chen, D.Q. Zhu, Adsorption of nonionic aromatic compounds to single-walled carbon nanotubes: effects of aqueous solution chemistry, Environ. Sci. Technol. 42 (2008) 7225–7230.
[3] B. Coasne, C. Alba-Simionesco, F. Audonnet, G. Dosseh, K.E. Gubbins, Adsorption, structure and dynamics of benzene in ordered and disordered porous carbons, Phys. Chem. Chem. Phys. 13 (2011) 3748–3757.
[4] F. El-Gohary, A. Tawfik, Decolorization, COD reduction of disperse and reactive dyes wastewater using chemical-coagulation followed by sequential batch reactor (SBR) process, Desalination 249 (2009) 1159–1164.
[5] A. Daas, O. Hamdaoui, Extraction of anionic dye from aqueous solutions by emulsion liquid membrane, J. Hazard. Mater. 178 (2010) 973–981.
[6] L. Wang, Aqueous organic dye discoloration induced by contact glow discharge electrolysis, J. Hazard. Mater. 171 (2009) 577–581.
[7] M.H. El-Naas, S.A. Al-Muhtaseb, S. Makhlouf, Biodegradation of phenol by *Pseudomonas putida* immobilized in polyvinyl alcohol (PVA) gel, J. Hazard. Mater. 164 (2009) 720–725.
[8] H.T. Gomes, B.F. Machado, A. Ribeiro, I. Moreira, M. Rosário, A.M.T. Silva, J.L. Figueiredo, J.L. Faria, Catalytic properties of carbon materials for wet oxidation of aniline, J. Hazard. Mater. 159 (2008) 420–426.
[9] T. Wu, X. Cai, S. Tan, H. Li, J. Liu, W.D. Yang, Adsorption characteristics of acrylonitrile, p-toluenesulfonic acid, 1-naphthalenesulfonic acid and methyl blue on graphene in aqueous solutions, Chem. Eng. J. 173 (2011) 144–149.
[10] S. Chakraborty, M.K. Purkait, S. DasGupta, S. De, J.K. Basu, Nanofiltration of textile plant effluent for color removal and reduction in COD, Sep. Purif. Technol. 31 (2) (2003) 141–151.
[11] V.K. Garg, R. Gupta, A.B. Yadav, R. Kumar, Dye removal from aqueous solution by adsorption on treated sawdust, Bioresour. Technol. 89 (2003) 121–124.
[12] S.J. Allen, G. McKay, J.F. Porter, Adsorption isotherm models for basic dye adsorption by peat in single and binary component systems, J. Colloid Interface Sci. 280 (2) (2004) 322–333.
[13] G. Crini, P.M. Badot, Application of chitosan, a natural aminopolysaccharide, for dye removal from aqueous solutions by adsorption processes using batch studies: a review of recent literature, Prog. Polym. Sci. 33 (2008) 399–477.
[14] Khalid Z.E. Lwakeel, Removal of reactive black 5 from aqueous solutions using magnetic chitosan resins, J. Hazard. Mater. 167 (2009) 383–392.
[15] G. Crini, Non-conventional low-cost adsorbents for dye removal: a review, Bioresour. Technol. 97 (2006) 1061–1085.
[16] S. Chatterjee, S.H. Woo, The removal of nitrate from aqueous solutions by chitosan hydrogel beads, J. Hazard. Mater. 164 (2009) 1012–1018.
[17] W.H. Cheung, Y.S. Szeto, G. McKay, Enhancing the adsorption capacities of acid dyes by chitosan nano particles, Bioresour. Technol. 100 (2009) 1143–1148.

[18] S. Wibowo, G. Velazquez, J. Savant, A. Torres, Surimi wash water treatment for protein recovery: effect of chitosan–alginate complex concentration and treatment time on protein adsorption, Bioresour. Technol. 96 (2005) 665–671.
[19] J.M. Wu, M.M. Luan, J.Y. Zhao, Trypsin immobilization by direct adsorption on metal ion chelated macroporous chitosan–silica gel beads, Int. J. Biol. Macromol. 39 (2006) 185–191.
[20] H.Y. Zhu, R. Jiang, L. Xiao, G.M. Zeng, Preparation, characterization, adsorption kinetics and thermodynamics of novel magnetic chitosan enwrapping nanosized α-Fe_2O_3 and multi-walled carbon nanotubes with enhanced adsorption properties for methyl orange, Bioresour. Technol. 101 (2010) 5063–5069.
[21] K.S. Novoselov, A.K. Geim, S.V. Morozov, D. Jiang, Y. Zhang, S.V. Dubonos, I.V. Grigorieva, A.A. Firsov, Electric field effect in atomically thin carbon films, Science 306 (2004) 666.
[22] C.N.R. Rao, A.K. Sood, K.S. Subrahmanyam, A. Govindaraj, Graphene the new two dimensional nanomaterial, Angew. Chem. Int. Ed. 48 (2009) 7752–7777.
[23] G.K. Ramesha, A. Vijaya Kumara, H.B. Muralidhara, S. Sampath, Graphene and graphene oxide as effective adsorbents toward anionic and cationic dyes, J. Colloid Interface Sci. 361 (2011) 270–277.
[24] N. Zhang, H. Qiu, Y. Si, W. Wang, J. Gao, Fabrication of highly porous biodegradable monoliths strengthened by graphene oxide and their adsorption of metal ions, Carbon 49 (2011) 827–837.
[25] P. Ramesh, S. Bhagyalakshmi, S. Sampath, Preparation and physicochemical and electrochemical characterization of exfoliated graphite oxide, J. Colloid Interface Sci. 274 (2004) 95.
[26] D. Depan, B. Girase, J.S. Shah, R.D.K. Misra, Structure–process–property relationship of the polar graphene oxide-mediated cellular response and stimulated growth of osteoblasts on hybrid chitosan network structure nanocomposite scaffolds, Acta Biomater. 7 (2011) 3432–3445.
[27] M. Sigomoto, M. Morimoto, H. Sashiwa, H. Saimoto, Y. Shigemasa, Preparation and characterization of water-soluble chitin and chitosan derivatives, Carbohydr. Polym. 36 (1998) 49–59.
[29] L. Zhou, et al., Adsorption of acid dyes from aqueous solutions by the ethylenediamine-modified magnetic chitosan nanoparticles, J. Hazard. Mater. 185 (2011) 1045–1052.
[30] M.J. Iqbal, M.N. Ashiq, Adsorption of dyes from aqueous solutions on activated charcoal, J. Hazard. Mater. B139 (2007) 57–66.